2016 IEEE 19th International Conference on Intelligent Transportation Systems (ITSC)
Windsor Oceanico Hotel, Rio de Janeiro, Brazil, November 1-4, 2016

Two-camera based accurate vehicle speed measurement using average speed at a fixed point

D. F. Llorca, C. Salinas, M. Jiménez, I. Parra, A. G. Morcillo, R. Izquierdo, J. Lorenzo, M. A. Sotelo

***Abstract*— In this paper we present a novel two-camera-based accurate vehicle speed detection system. Two high-resolution cameras, with high-speed and narrow field of view, are mounted on a fixed pole. Using different focal lengths and orientations, each camera points to a different stretch of the road. Unlike standard average speed cameras, where the cameras are separated by several kilometers and the errors in measurement of distance can be in the order of several meters, our approach deals with a short stretch of a few meters, which involves a challenging scenario where distance estimation errors should be in the order of centimeters. The relative distance of the vehicles w.r.t. the cameras is computed using the license plate as a known reference. We demonstrate that there is a specific geometry between the cameras that minimizes the speed error. The system was tested on a real scenario using a vehicle equipped with DGPS to compute ground truth speed values. The obtained results validate the proposal with maximum speed errors $< 3kmh$ at speeds up to $80kmh$.**

***Index Terms*— Vehicle speed measurement, average speed, range error, speed error, license plate.**

I. INTRODUCTION

According to the Global Status Report on Road Safety 2015 by the WHO [1], the speed limit on a section of road takes account of safety, mobility and environmental considerations. Enforcement of speed limits is essential to make them truly effective. Indeed, the WHO [1] proposes to increase emphasis on enforcement of speed limits in most countries for successfully developing safer driving behavior. A recent review of 35 studies [2] found that, in the vicinity of speed cameras, the typical range of reduction in the proportion of speeding vehicles was in the 10-35% and the typical crash reductions was of 14-25%. Accordingly, accurate speed detection of moving vehicles is a key issue to traffic law enforcement in most countries that may lead to an effective reduction in the number of road accidents and fatalities.

Depending on the methodology employed for the estimation, vehicle speed measurement procedures can be categorized as instantaneous or average speed. On the one hand, instantaneous approaches measure the speed at a single point. They are usually based on laser (time of flight) or radar (Doppler effect) technologies as well as sensors (inductive or piezo electronic) embedded in pairs under the road surface. These sensors are placed at a fixed position. They also require a camera to document speed violations. On the other hand, average speed approaches make use of at least two cameras at a minimum of hundreds of meters apart (usually $> 1km$).

D. F. Llorca, C. Salinas, M. Jiménez, I. Parra, A. G. Morcillo, R. Izquierdo, J. Lorenzo, M. A. Sotelo are with the Computer Engineering Department, Polytechnic School, University of Alcalá, Madrid, Spain. email: david.fernandezl@uah.es.

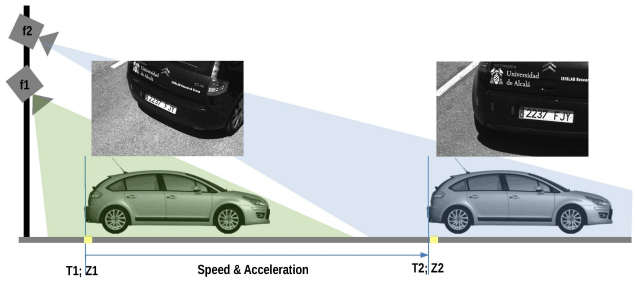

Fig. 1. Overall view of the proposed two-camera based vehicle speed measurement at a fixed location.

As vehicles pass between the cameras they are digitally recorded. The time it takes for the vehicle to travel between both points is used to calculate the average speed.

There are a considerable number of commercial systems based on the aforementioned methods that fulfill the high standards of accuracy required by national metrology authorities to approve the use of a speed measurement system to enforce speed limits (Spain case [3]: speed error $< \pm 3kmh$ up to $100kmh$, and $< \pm 3\%$ at speeds $> 100kmh$). However, besides average speed procedures, the number of vision-based commercial solutions located at a fixed point (instantaneous or average speed), certified by national authorities is very limited due to intrinsic limitations of computer vision approaches such as sensor discretization and perspective distortion. As an example, in Spain, at present there are not fixed vision-based vehicle speed detection commercial systems certified by the national metrology agency [3].

In this paper we present a novel two-camera based vehicle speed detection system. It estimates the speed of a vehicle using pairs of distance measurements obtained from two high-resolution and high-speed cameras, with a narrow field of view, different focal length and orientation. Thus, each camera points to a different stretch of the road (see Fig. 1). We demonstrate that there is a specific geometry between the cameras that provides pairs of relative distance values that minimize the speed error. A known reference (width of the license plate) is used to compute relative distance measurements. The proposal is directly focused on minimizing the maximum speed error within the limits determined by the regulatory authorities of most countries.

II. RELATED WORK

Bounds on vision-based distance and speed estimation accuracy were analytically and experimentally studied in 2003 in [4]. The conclusions were clear: the range error increases

quadratically with the distance and linearly with the pixel error; the speed error increases linearly with the distance and the vehicle speed, and decreases linearly with the focal length (in pixels) and the time window (or the length of the segment used to compute the speed). In addition, the effect of a constant acceleration when computing the speed taking the range difference at two different frames adds a linear term to the speed error which can be minimized computing an optimal time window, producing a speed error that increases linearly with the range.

Accordingly, the design of a precise vision-based vehicle speed measurement system should involve several key points: the use of very large focal lengths (narrow field of view) and high resolution sensors with small pixel size, the detection of the vehicle as close as possible (small ranges) and the use of optimal time windows or length between two measurements. However, the literature review on this field corroborates that these important issues have been somehow neglected. Most of the approaches are applied on images recorded by traffic cameras, covering two lanes or more, with VGA resolution or similar, low/medium focal lengths, and detecting the vehicles at very large distances w.r.t. the cameras [5], [6], [7], [8], [9], [10], [11], [12], [13], [14], [15], [16], [17], [18], [19]. Some exceptions can be found in [20] and [21]. In addition, in most cases the speed is computed in a frame-by-frame fashion (instantaneous) [5], [6], [7], [9], [10], [11], [12], [22], [14], [15], [20], [18], [19], [21] without taking into account that the range error can be of a similar order of magnitude than the range difference at two consecutive frames, and considering that the vehicle has zero acceleration. Only a few works proposed to estimate the vehicle speed using two non-consecutive points [8], [13],[16], [17].

From the methodological point of view, the most common approach consist in segmenting the vehicles using background subtraction, frame differencing or Adaboost techniques, tracking them using blob detection, correlation or filtering methods, with the speed being estimated from the displacement of the contact point of the vehicle with the road using inverse perspective mapping, or flat world assumption, and a scale factor in $meters/pixel$ obtained after camera calibration [5], [6], [7], [9], [10], [11], [12], [13], [14], [15], [16], [17], [19]. The use of optical flow vectors transformed to space magnitudes after camera calibration has been used in [22] with side view images and in [18] with traffic images. The detection and tracking of the license plate to estimate the relative movements of the vehicles was proposed in [23] with one blurred image, and in [20] and [21] to use stable features for vehicle tracking.

The validation of the different methodologies is far from being homogeneous. Some works reported traffic speed results rather than vehicle speed ones [5], [6]. In many cases the reported results were not compared with a speed ground truth [7], [11], [23], [14], [16]. The use of the car speedometer to measure the ground truth speed, proposed in [15] and [17], involves some inaccuracies due to the fact that most car manufactures intentionally bias it. Other approaches make use of radar [9], [18], standard GPS [12], [22], GPS speedometer on-board of the vehicle [19], [21], light-barriers [8] and in-pavement sensors, such as fiber optic [13] or inductive loops [20].

III. SYSTEM DESCRIPTION

A. System Layout

As can be seen in Fig. 1, two cameras with different focal length and orientation are mounted on a fixed pole pointing to different stretch of the road. The average vehicle speed is computed using pairs of relative distance measurements from both cameras. Vehicle detections are separated by a few meters unlike standard average speed cameras where these ones are separated by kilometers. Since the range error increases quadratically with the distance, and due to the narrow field of view of the lens, the system has been designed for monitoring one single lane (multiple lanes would require multiple systems). The overall architecture is shown in Fig. 2. It is composed of two CMOS USB 3.0, with a 1920×1200 pixel resolution, and a maximum frame rate of 160 FPS. The first camera has a focal length of $25mm$ and it is configured to detect the license plate of the vehicle as close as possible to minimize both range and pixel localization errors. The second camera has focal focal length of $75mm$ pointing to a second stretch (not overlapped w.r.t. the first camera) at a distance that will be defined according to a specific geometry that minimizes the speed error. A specific synchronization HW controls both the external trigger and the exposure time of the cameras. A PPS GPS receiver with USB interface that advertises NMEA-0183 compliance is used to run a NTP server (stratum 1) corrected by a GPSD time service. Thus, highly accurate timestamps can be provided to compute the vehicle speed and to synchronize the data of the vision system with the DGPS measurements on the test vehicle.

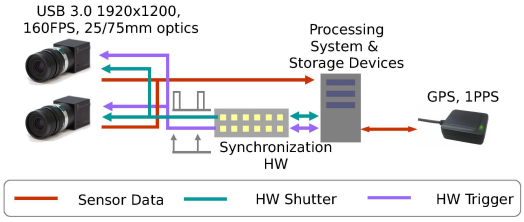

Fig. 2. Sensor architecture.

The overall speed detection procedure (see Fig. 3) consists of several stages. First, the system installation and cameras calibration, including the extrinsic relationship w.r.t. the road plane, are carried out. The system is run once the vehicle license plate is located by the first camera, and stopped once it is not visible by the second one. For each camera and each frame, the license plate is localized and its relative distance to each camera is computed and stored, including the corresponding timestamp. Finally, we optimally pair all the available range and time measurements between both cameras selecting the ones that fullfill with the requirements of a pre-computed geometry that minimizes the speed error and combining them to estimate the final vehicle speed.

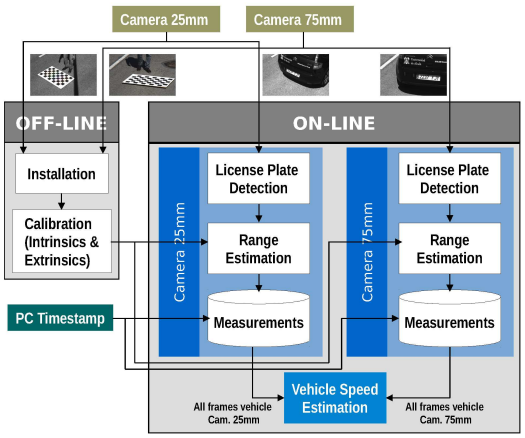

Fig. 3. Flowchart representation of the overall approach.

B. Speed Error Fundamentals

Average vehicle speed cameras are located in at least two locations at a minimum of hundreds of meters apart. The speed error provided by these approaches decreases linearly with the length of the stretch. Accordingly, most of the commercial systems are designed to be used over a set distance of several kilometers. In a simple scenario, given two locations Z_1 and Z_2 (the stretch will be $S = Z_2 - Z_1$) of a vehicle detected at times t_1 and t_2 ($\Delta t = t_2 - t_1$) respectively, the average speed will be $v = (Z_2 - Z_1)/(t_2 - t_1)$ (or $v = S/\Delta t$. Now, if we consider localization errors Z_{1err} and Z_{2err}, the worst case scenario will provide an estimated speed of $v' = (S + Z_{2err} + Z_{1err})/\Delta t$ with the following speed error:

$$v_{err} = v' - v = \frac{Z_{2err} + Z_{1err}}{\Delta t} = \frac{Z_{2err} + Z_{1err}}{S} v \qquad (1)$$

being the relative speed error $v_{err}/v = (Z_{2err} + Z_{1err})/S$. License Plate Recognition (LPR) systems are usually able to localize license plates in ranges that may vary between $5 - 15m$ depending on the application. Accordingly, in practice, there is no need to estimate the relative position of the vehicle w.r.t. the camera if the length of the stretch is large enough. For instance, if $S = 1km$ we can manage localization errors of up to $15m$ at each camera position, and the relative speed error will be lower than 3%. The challenge of our approach is that the length of the stretch (a few meters) involves localization errors in the order of *cms*. As an example, for $S = 6m$, localization errors should be lower than $9cm$ at each position to obtain a relative speed error lower than 3%.

In order to analyze the range error in more detail, we consider a simple scenario where the camera is directly placed at the road plane reference (see Figs. 4(a) and 4(b)), the images are undistorted, and the range is computed using the width of the license plate. The width of the license plate $\Delta X = X_2 - X_1$ in world coordinates is a known parameter. After camera calibration we know the focal length in pixels $f_x = f/d_x$ (f focal length in *mm*, and d_x the pixel size). After applying a license plate localization method, the width of the license plate can be obtained at the image plane in pixels $\Delta u = u_2 - u_1$. Considering the license plate as a plane that moves towards the Z axis, its distance to the camera can be computed as $Z = f_x(\Delta X/\Delta u)$. Even if the pixel localization error is zero, the image discretization involves a discretization error represented by the size of each pixel in world coordinates $D_x = (Z/f)d_x = Z/f_x$. Being n the pixel localization error of the projected license plate, the worst case scenario would provide a distance value of $Z' = f_x(\Delta X + nD_x)/\Delta u$. Thus, the range error will be:

$$Z_{err} = Z' - Z = f_x \frac{nD_x}{\Delta u} = \frac{nZ}{\Delta u} = \frac{nZ^2}{f_x \Delta X} \qquad (2)$$

Merging Eq. (1) with Eq. (2) we have the following speed error:

$$v_{err} = \frac{\frac{n_1 Z_1^2}{f_{x1}\Delta X} + \frac{n_2 Z_2^2}{f_{x2}\Delta X}}{Z_2 - Z_1} v \qquad (3)$$

where n_1 and n_2 are the pixel localization errors of both cameras, and f_{x1} and f_{x2} are the focal length in pixels of both cameras. Note that if the road stretch begins at $Z_1 = 0$, the speed error increases linearly with the distance to the second point Z_2. However, if $Z_1 \neq 0$, Eq. (3) involves a quadratic curve that will mainly depend on v, Z_1 and Z_2.

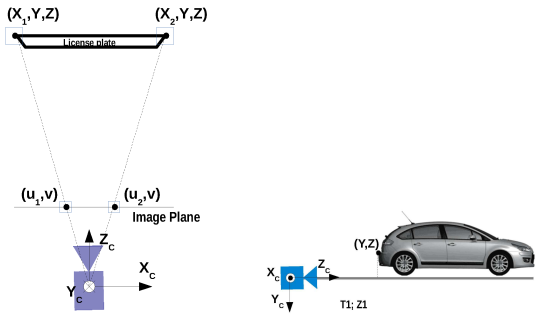

Fig. 4. Simple scenario to analyze range errors. (a) Top view. (b) Lateral view.

In Fig. 5(a) we show the speed error using Eq. (3), for a fixed $Z_1 = 3m$, Z_2 values from $0 - 55m$ at speeds from $20 - 100kmh$. The simulation shows that the speed error linearly increases with the vehicle speed. The obtained curves show a minimum value from which the speed error increases linearly with the distance Z_2. However, the most important conclusion is that, for a fixed Z_1, there is an optimal value of Z_2 that provides the minimum speed error independently of the speed of the vehicle. As can be observed in Fig. 5(b), for a fixed vehicle speed, different values of Z_1 will involve different optimal Z_2 values. Therefore, for a known Z_1 we can find an optimal $\hat{Z}_2$ which minimizes the speed error by differentiating Eq. (3) w.r.t. Z_2 and setting it to zero:

$$\frac{\partial v_{err}}{\partial Z_2} = \ldots = (n_2 f_{x1})Z_2^2 - (2n_2 f_{x1} Z_1)Z_2 - n_1 f_{x2} Z_1^2 = 0 \qquad (4)$$

We can now solve Eq. (4) for Z_2:

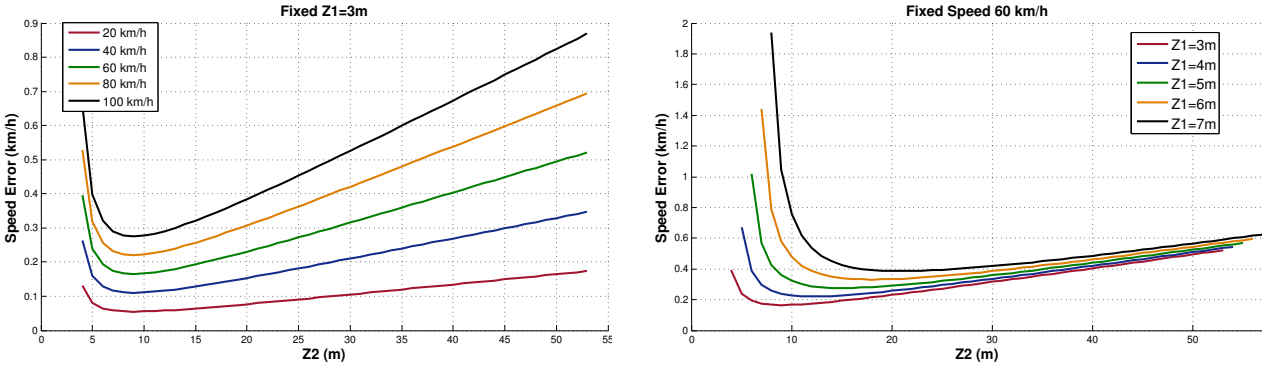

(a) (b)

Fig. 5. Speed error along Z_2. (a) Fixed Z_1 and different vehicle speeds. (b) Fixed vehicle speed and different Z_1 values.

$$\hat{Z}_2 = \frac{Z_1(n_2 f_{x1} + \sqrt{n_2^2 f_{x1}^2 + n_1 n_2 f_{x1} f_{x2}})}{n_2 f_{x1}} \tag{5}$$

Although this error analysis has been derived from a simple and unrealistic scenario (Fig. 4), the conclusions can be extended to the real one (Fig. 1) by taking into account extrinsic calibration (rotation and translation) errors between the road plane and the camera reference. Eq. (5) will be used to define the rotation of the cameras at *Installation* stage (see Fig. 3), so that the measurements taken at the first position could be optimally paired with measurements at the second one. Then, Eq. 5 will be also applied to only allow optimal matches, i. e., measurements Z_1 and Z_2 that accomplish the Eq. 5, to be used when computing the vehicle speed. Thus, we can assure that the speed error will be minimized.

C. Vehicle Speed Estimation

1) License Plate Localization: As described in previous section, we use the license plate to compute the range of the vehicle since we have knowledge of its standard dimensions in world coordinates. A global overview of our license plate localization approach is depicted in Fig. 6. As can be observed we make use of a combination of the MSER [24] and SWT [25] detectors to isolate the characters regions according to some filtering criteria (size, relative positions, etc.). The final character regions are used to perform a fine-tuned search of the license plate borders using the probabilistic Hough transform [26], computing the intersection points between the most prominent horizontal and vertical lines, and correcting them using the corner detector algorithm described in [27]. A specific OCR (Optical Character Recognition) based on CNN (Convolutional Neural Networks) is finally applied to assure that the vehicle captured by both cameras is the same.

2) Relative Range Estimation: The overall setup used to estimate the relative range of the vehicle is depicted in Fig. 7. As can be observed, each camera points to a different region and needs to be extrinsically calibrated. Using a chessboard calibration pattern we obtain the relative rotation and translation (R_i, T_i with $i = 25$ for the first camera and $i =$ 75 for the second one) to convert points from the world/road reference to the camera reference. The calibration process is defined assuring that the rotation between road references of both cameras is the identity matrix. Then, after license plate localization we estimate the relative distance of it w.r.t. to the world reference by using the lower corners ($p_1 = (u_i^1, v_i^1)$ and $p_2 = (u_i^2, v_i^2)$), and considering that the height Y_{wi} of both corners is the same. In addition, we have previous knowledge of the distance between both corners in world coordinates ΔX. Considering K_i the intrinsic calibration matrix, and using homogeneous coordinates, the projection of each 3D point onto the image plane can be written as:

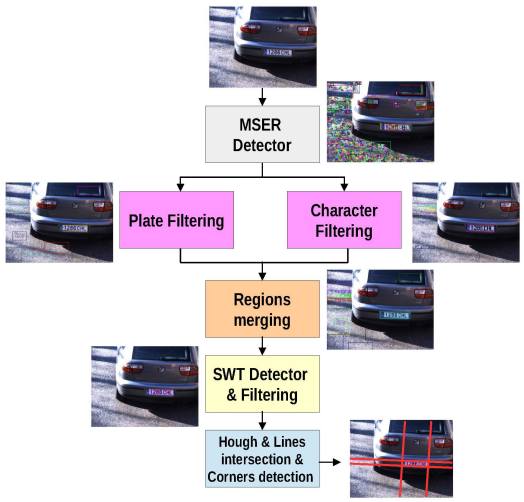

Fig. 6. Global overview of our license plate localization system.

$$sp_i = s \begin{pmatrix} u_i \\ v_i \\ 1 \end{pmatrix} = [K_i|0_3] \begin{bmatrix} R & T \\ 0_3^T & 1 \end{bmatrix} \begin{pmatrix} X_{wi} \\ Y_{wi} \\ Z_{wi} \\ 1 \end{pmatrix} = M_i P_{wi} \tag{6}$$

Then we define the following set of equations:

$$sp_i^1 = M_i P_{wi}^1 \tag{7}$$

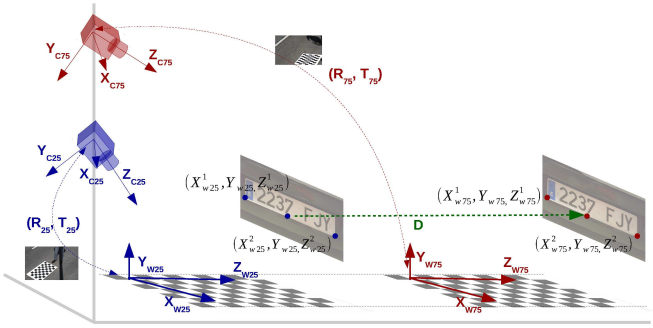

Fig. 7. Relative positions between cameras and world plane and license plate points.

$$sp_i^2 = M_i P_{wi}^2 \tag{8}$$

$$X_{wi}^2 - X_{wi}^1 = \Delta X \tag{9}$$

that can be rearranged as in the linear form $Ax = b$, being A a 5×5 matrix, b a 5×1 vector and $x = (X_{wi}^1, X_{wi}^2, Y_{wi}, Z_{wi}^1, Z_{wi}^2)$. Since A is square and has full rank, the system has a unique solution given by $x = A^{-1}b$. In order to manage one unique point, we compute the average value of both corners at each camera, so the final point $P_{wi} = ((X_{wi}^2 + X_{wi}^1)/2, Y_{wi}, (Z_{wi}^2 + Z_{wi}^1)/2)$ will correspond to the lower middle region of the license plate.

Finally, the relative coordinates of points P_{wi} are translated to the camera reference but maintaining their orientation w.r.t. to the road reference, i.e.:

$$P'_{c25} = P_{w25} + R_{25}^{-1} T_{25} \tag{10}$$

$$P'_{c75} = P_{w75} + R_{75}^{-1} T_{75} \tag{11}$$

The final range measurement that represents the displacement of the lower middle point of the license plate between both cameras is computed as:

$$D = \|P'_{c75} - P'_{c25}\| \tag{12}$$

3) Speed Measurement: The proposed approach is based on high-speed cameras (160 FPS). Accordingly, for each vehicle and depending on its speed we can have around hundreds of measurements at each camera. However, not all of them are used to compute the vehicle speed. Eq. 12 is only applied between pairs of measurements P'_{c75} and P'_{c25} that fulfill the restriction defined in Eq. 5 to guarantee minimum speed errors. In addition, we have an accurate timestamp for each measurement because of the NTP server installed on the PC. Let's consider $j = 1 \ldots N$ the number of optimal pairs of measurements P'^j_{c75} and P'^j_{c25} that yield the displacements D^j, and t^j_{25} and t^j_{75} the corresponding timestamps. Then, the final vehicle speed estimation is given by:

$$V = \frac{1}{N} \sum_{j=1}^{N} \frac{D^j}{t^j_{75} - t^j_{25}} \tag{13}$$

IV. EXPERIMENTS

In order to validate the proposed approach, we have devised a test scenario at the Campus University of Alcalá, using our fully autonomous vehicle, equipped with RTK-DGPS sensor (see Fig. 8), NTP-GPSD time service, and CAN Bus connectivity, among other sensors and actuators. The $25mm$ and the $75mm$ cameras cover a region centered at $3m$ and $9m$ respectively to accomplish with Eq. (5). The speed ground truth is obtained from the DGPS sensor by using Northing-Easting measurements with a positional accuracy of $2.5cm$, which for the stretch of $6m$ involves relative speed errors $< 0.83\%$. Since the DGPS provides data at $20Hz$ and the cameras work at $160Hz$, DGPS measurements were linearly interpolated to be synchronized with each frame of the camera, using the accurate PC timestamps that are given by the NTP client corrected by the GPSD time service.

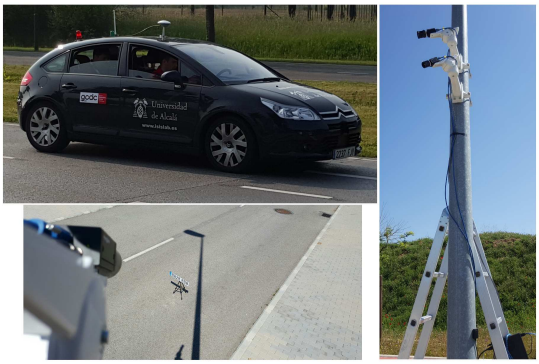

Fig. 8. Test scenario including the vehicle used during the experiments, and the cameras.

An experienced driver was requested to drive at a predefined fixed speed making use of the speed controller of the vehicle when possible. Eight different runs were made at eight different speeds $\{10,20,30,40,50,60,70,80\}kmh$ approximately. Speed errors were computed using ground truth data from the DGPS. In Table I we show the mean absolute speed error, the standard deviation and the maximum absolute error for each of the speeds. Note that the first column only shows the approximate speed of each of the eight runs. As can be observed, maximum errors are within $\pm3kmh$ in all cases. The mean absolute speed error corresponding to all runs is $1.44kmh$ which clearly validates the proposed methodology. In addition, if we do not consider optimal pairs of measurements between both cameras following the Eq. (5) the mean absolute error is $1kmh$ larger aproximately, in some cases $> 3kmh$. As an example in Fig. 9 we show the raw speed measurements for a run of $80kmh$, the DPGS ground truth speed, the speed computed by averaging all measurements, and the speed using only optimal pairs of measurements. As can be observed, the error is clearly reduced.

V. CONCLUSION

We have presented a novel two-camera-based approach to perform highly accurate vehicle speed estimation. High-resolution and high-speed cameras with a narrow field of

TABLE I

VEHICLE SPEED ESTIMATION RESULTS IN KMH.

Aprox. Speed	Mean. Abs. Err.	Std.	Max. Err.
10	0.90	0.31	1.24
20	1.28	0.27	1.51
30	1.76	0.16	1.92
40	1.63	0.27	2.01
50	1.66	0.50	2.17
60	1.70	0.81	2.62
70	0.45	0.17	0.63
80	2.13	0.41	2.52

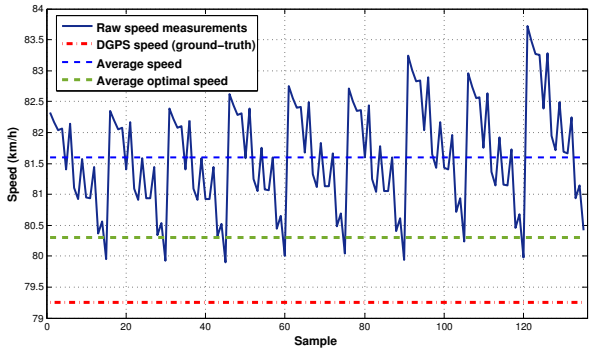

Fig. 9. Example at 80*kmh*. Raw speed measurements, DGPS ground truth, average speed value with all measurements, and average speed value with optimal pairs of measurements. The periodicity of the curve is not relevant since it is related with the way the pairs of measurement between both cameras are stored.

view, different focal length and orientation are mounted on a fixed pole, pointing to two different stretch of the same road lane. We have proved that there is a specific geometry between the cameras that minimize the speed error. In our experiments, we have obtained a mean absolute speed error of 1.44*kmh* for speeds up to 80*kmh*. In all cases, the maximum speed error is always $< 3kmh$. These are encouraging results that validate our methodology. Future works will involve extensive validation, including nighttime scenarios and comparisons with other approaches.

VI. ACKNOWLEDGMENTS

This work was supported by the Research Grants VISPEED SPIP2015-01737 (General Traffic Division of Spain), IMPROVE DPI2014-59276-R (Spanish Ministry of Economy), and SEGVAUTO-TRIES-CM S2013/MIT-2713 (Community of Madrid).

REFERENCES

[1] WHO, "Global status report on road safety," 2015, site: http://www.who.int/violence_injury_prevention/road_safety_status/2015/.

[2] C. Wilson, C. Willis, J. K. Hendrikz, R. L. Brocque, and N. Bellamy, "Speed cameras for the prevention of road traffic injuries and deaths," *Cochrane Database of Systematic Reviews*, vol. 11, no. CD004607, 2010.

[3] CEM, "Centro español de metrología, certificado de examen de modelo," 2016, site: http://www.cem.es/content/ex%C3%A1menes-de-modelos?term_node_tid_depth=139.

[4] G. P. Stein, O. Mano, and A. Shashua, "Vision-based acc with a single camera: Bounds on range and range rate accuracy," in *IV2003, IEEE Intelligent Vehicle Symposium*, 2003.

[5] T. N. Schoepflin and D. J. Dailey, "Dynamic camera calibration of roadside traffic management cameras for vehicle speed estimation," *IEEE Transactions on Intelligent Transportation Systems*, vol. 4, no. 2, pp. 90–98, 2003.

[6] F. W. Cathey and D. J. Dailey, "A novel technique to dynamically measure vehicle speed using uncalibrated roadway cameras," in *IV2005, IEEE Intelligent Vehicle Symposium*, 2005.

[7] L. Grammatikopoulos, G. Karras, and E. Petsa, "Automatic estimation of vehicle speed from uncalibrated video sequences," in *International Symposium on Modern Technologies, Education and Professional Practice in Geodesy and Related Fields*, 2005.

[8] D. Bauer, A. N. Belbachir, N. Donath, G. Gritsch, B. Kohn, M. Litzenberger, C. Posch, P. Schon, and S. Schraml, "Embedded vehicle speed estimation system using an asynchronous temporal contrast vision sensor," *EURASIP Journal on Embedded Systems*, vol. 82174, 2007.

[9] X. C. He and N. H. C. Yung, "A novel algorithm for estimating vehicle speed from two consecutive images," in *IEEE Workshop on Applications of Computer Vision (WACV07)*, 2007.

[10] B. Alefs and D. Schreiber, "Accurate speed measurement from vehicle trajectories using adaboost detection and robust template tracking," in *IEEE Intelligent Transportation Systems Conference (ITSC))*, 2007.

[11] H. Zhiwei, L. Yuanyuan, and Y. Xueyi, "Models of vehicle speeds measurement with a single camera," in *International Conference on Computational Intelligence and Security Workshops*, 2007.

[12] C. Maduro, K. Batista, P. Peixoto, and J. Batista, "Estimation of vehicle velocity and traffic intensity using rectified images," in *IEEE International Conference on Image Processing*, 2008.

[13] T. Celik and H. Kusetogullari, "Solar-powered automated road surveillance system for speed violation detection," *IEEE Transactions on Industrial Electronics*, vol. 57, no. 9, pp. 3216–3227, 2010.

[14] H. A. Rahim, U. U. Sheikh, R. B. Ahmad, and A. S. M. Zain, "Vehicle velocity estimation for traffic surveillance system," *International Journal of Computer, Electrical, Automation, Control and Information Engineering*, vol. 4, no. 9, pp. 1465–1468, 2010.

[15] T. T. Nguyen, X. D. Pham, J. H. Song, S. Jin, D. Kim, and J. W. Jeon, "Compensating background for noise due to camera vibration in uncalibrated-camera-based vehicle speed measurement system," *IEEE Transactions on Vehicular Technology*, vol. 60, no. 1, pp. 30–43, 2011.

[16] O. Ibrahim, H. ElGendy, and A. M. ElShafee, "Speed detection camera system using image processing techniques on video streams," *International Journal of Computer and Electrical Engineering*, vol. 3, no. 6, pp. 711–778, 2011.

[17] Z. Shen, S. Zhou, C. Miao, and Y.Zhang, "Vehicle speed detection based on video at urban intersection," *Research Journal of Applied Sciences, Engineering and Technology*, vol. 5, no. 17, pp. 4336–4342, 2013.

[18] J. Lan, J. Li, G. Hu, B. Ran, and L. Wang, "Vehicle speed measurement based on gray constraint optical flow algorithm," *Optik*, vol. 125, pp. 289–295, 2014.

[19] Y. G. A. Rao, N. S. Kumar, S. H. Amaresh, and H. V. Chirag, "Real-time speed estimation of vehicles from uncalibrated view-independent traffic cameras," in *IEEE Region 10 Conference TENCON*, 2015.

[20] D. C. Luvizon, B. T. Nassu, and R. Minneto, "Vehicle speed estimation by license plate detection and tracking," in *IEEE International Conference on Acoustics, Speech and Signal Processing (ICASSP)*, 2014.

[21] C. Ginzburg, A. Raphael, and D. Weinshall, "A cheap system for vehicle speed detection," in *preprint arXiv:1501.06751*, 2015.

[22] S. Dogan, M. S. Temiz, and S. Kulur, "Real time speed estimation of moving vehicles from side view images from an uncalibrated video camera," *Sensors*, vol. 10, pp. 4805–4824, 2010.

[23] H.-Y. Lin, K.-J. Li, and C.-H. Chang, "Vehicle speed detection from a single motion blurred image," *Image and Vision Computing*, vol. 26, pp. 1327–1337, 2008.

[24] J. Matas, O. Chum, M. Urban, and T. Pajdla, "Robust wide-baseline stereo from maximally stable extremal regions," *Image and vision computing*, vol. 22, no. 10, pp. 761–767, 2004.

[25] B. Epshtein, E. Ofek, and Y. Wexler, "Detecting text in natural scenes with stroke width transform," in *Computer Vision and Pattern Recognition (CVPR)*, 2010.

[26] J. Matas, C. Galambos, and J. V. Kittler, "Robust detection of lines using the progressive probabilistic hough transform," *Computer Vision and Image Understanding*, vol. 78, no. 1, pp. 119–137, 2000.

[27] J. Shi and C. Tomasi, "Good features to track," in *Computer Vision and Pattern Recognition (CVPR)*, 1994.